eprints@whiterose.ac.uk
https://eprints.whiterose.ac.uk/

The stabilization and release performances of curcumin-loaded liposomes coated

by high and low molecular weight chitosan

Kedong Tai [a], Michael Rappolt [b], Like Mao [a], Yanxiang Gao [a], Xin Li [c], Fang Yuan [a,*]

[a] Beijing Advanced Innovation Center for Food Nutrition and Human Health, Beijing Laboratory for Food Quality and Safety, Beijing Key Laboratory of Functional Food from Plant Resources, College of Food Science & Nutritional Engineering, China Agricultural University, Beijing 100083, P.R. China

[b] School of Food Science and Nutrition, University of Leeds, Leeds LS2 9JT, U.K.

[c] School of Food Science, Jiangnan University, Wuxi, Jiangsu, 214122, P.R. China

*Corresponding author (Fang Yuan).

Tel: +86-10-62737034

Address: Box 112, No.17 Qinghua East Road, Haidian District, Beijing 100083, China

E-mail: yuanfang0220@cau.edu.cn

22 **ABSTRACT**

23 A comprehensive stability evaluation for curcumin-loaded liposomes (Cur-LP)

24 coated by low (LCS) or high (HCS) molecular weight chitosan with three gradient

25 concentrations (L: low; M: medium; H: high) was the main objective of this study.

26 Apart from leading to a higher encapsulation efficiency (> 90%), all chitosan-coated

27 Cur-LP displayed an improved stability with respect to resistant to salt, sunlight, heat,

28 accelerated centrifugation and long-term storage at 4 °C. Increasing the molecular

29 weight and concentration of chitosan could effectively improve the stability of Cur-LP,

30 in which HCS-H coatings displayed the best performance. According to the

31 fluorescence probe analysis, the mechanical reinforcement of liposomes and the

32 concomitant reduction in membrane fluidity accounts for the major contribution to

33 vesicle stability. Secondly, a simulated digestion model was used to prove the

34 applicability of sustained curcumin release, achieved by adjusting the molecular weight

35 and concentration of the chitosan stabilizer for Cur-LP. The results of this study show

36 that high molecular weight chitosan used at relatively high concentrations, is a

37 promising coating material for improving the stability and sustained release of Cur-LP

38 *in vitro*.

39 **KEYWORDS:** liposomes; curcumin; chitosan; vesicle stability; sustained release
40

1. Introduction

In recent years, the bioactive properties of curcumin have been widely investigated, including antioxidant, anti-inflammatory, antimicrobial and anticarcinogenic activities (Anand, Kunnumakkara, Newman, & Aggarwal, 2007). Curcumin is a hydrophobic polyphenol extracted from the rhizome of herb *Curcuma longa*. Although it has been used as traditional Chinese medicine for centuries, three principle limitations were not addressed until modern medical studies have focussed on this bioactive compound: (ⅰ) low solubility, (ⅱ) easy degradability and (ⅲ) poor bioavailability (Nelson, et al., 2017). As a matter of fact, the hydrophobicity and rapid metabolism of curcumin are the main culprits, preventing people from to benefit from it. In fact, its bioavailability reaches only 1% after oral administration (Liu et al., 2016). Several delivery strategies have been employed to overcome these obstacles, such as designing emulsions (Ma, et al., 2017), micelles (Wang & Gao, 2018), hydrogels (Zheng, Zhang, Chen, Luo, & McClements, 2017) , nanoparticles (C. Tan, Xie, Zhang, Cai, & Xia, 2016), applying electrospun fibres (Alehosseini, Gomez-Mascaraque, Martinez-Sanz, & Lopez-Rubio, 2019), creating phospholipid complexes (Maiti, Mukherjee, Gantait, Saha, & Mukherjee, 2007) and using liposomal systems (Alavi, Haeri, & Dadashzadeh, 2017; Karewicz et al., 2013; Liu, Liu, Zhu, Gan, & Le, 2015; Pu, Tang, Li, Li, & Sun, 2019). From nutrition and safety perspectives, liposome are recognized having great potential as nutraceutical carriers. They form by self-assembly of commonly used phospholipid molecules, and display an onion-like architecture consisting of altering lipid and water

62 layers with a central water core. These liposomes are also known as multi-lamellar

63 vesicles (MLVs), or when only bilayer is given, as unilamellar vesicles (ULVs). In spite

64 of biocompatibility, biodegradability, nontoxicity, and non-immunogenicity as

65 advantages for liposomes (Li et al., 2019), their bad physicochemical stability severely

66 limits the application in the food industry as well as in pharmacy. One reason for poor

67 stability lies in the high sensitivity to chemical degradation of phospholipids by

68 hydrolysis of the ester groups and oxidation of unsaturated acyl chains, which facilitate

69 the structural disruption of liposomal membranes. Another reason for poor stability is

70 caused by vesicle fusion, which induces larger vesicles and sedimentation. Finally, the

71 phase separation of hydrophobic bioactive compounds from lipid bilayer can occur due

72 to lipid degradation and/or temperature fluctuations, which also leads to the leakage of

73 the embedded bioactive compounds (Grit & Crommelin, 1993). Thus, how to decrease

74 the susceptibility to environmental stress and achieve an efficient utilization liposomes

75 is still attracting growing interest.

76   Compared with tedious protocols for modifying the composition of liposomal

77 membranes, surface coating has been identified as economical and effective method to

78 improve stability (He et al., 2019). Among numerous coating materials, chitosan is a

79 well-considered choice to form protective polyelectrolyte layers due to the positive

80 charges that readily interact with negatively charged liposomal surfaces. In addition,

81 the biocompatible and biodegradable polysaccharides have been permitted to be used

82 in food products, such as for antimicrobial and preservative films applied in food

83 storage (Mujtaba et al., 2019). The chitosan-coating method has been proposed many

84 years ago (Henriksen, Smistad, & Karlsen, 1994; Henriksen, Vagen, Sande, Smistad,

85 & Karlsen, 1997) and has been applied in several bioactive compounds-loaded

86 liposomes in recent years, concerning the up-take of resveratrol (Park, Jo, & Jeon, 2014),

87 quercetin (Hao et al., 2017), peptides (Gradauer et al., 2013), and curcumin (Karewicz

88 et al., 2013; Li et al., 2017; Liu et al., 2015). Nevertheless, we note that nearly all studies

89 have focused on only one type of chitosan or on its modified derivative. Apart from its

90 stabilization properties, Cuomo et al. found that chitosan coating could also

91 significantly improve the absorption of curcumin in liposomes, shown by *in vitro*

92 digestion analysis (Cuomo et al., 2018). This is mainly attributed to the improvement

93 of mucoadhesive properties of chitosan-coated vesicles (Shin, Chung, Kim, Joung, &

94 Park, 2013). Further, study focusing on the thermal stability comparison between

95 chitosan-coated and uncoated Cur-LP, demonstrated that chitosan coatings effectively

96 protect curcumin from degradation and drastically reduce leakage (Liu et al., 2015). As

97 to chitosan derivatives, Tian et al. studied the potential of carboxymethyl and

98 quaternary ammonium chitosan-coated liposomes and found that the chitosan

99 derivatives-coated liposomes displayed a six folds higher bioavailability of curcumin

100 after oral administration, when compared to uncoated ones (Tian et al., 2018). Thiolated

101 chitosan was also synthesized to be applied in Cur-LP, which led to a slower *in vitro*

102 release and a higher stability above room temperature (Li et al., 2017). Apart from

103 single-layered chitosan coatings utilized in the above studies, multi-layered chitosan

coatings were also formed to evaluate the protective efficacy for liposomes (Jeon, Yoo, & Park, 2015). Layer-by-layer coatings were prepared by electrostatic deposition of positively charged chitosan and other negatively charged polyelectrolytes. Also these stabilised liposomes exhibited an improved sustained release property for embedded bioactive compounds.

With respect to the different molecular properties of chitosan on liposomes, previous studies have revealed that increasing the molecular weight and concentration improved physical stability of liposomes to some extent (Filipovic-Grcic, Skalko-Basnet, & Jalsenjak, 2001; Laye, McClements, & Weiss, 2008), as well as improved the hypoglycaemic efficacy after oral administration in mice (Wu, Ping, Wei, & Lai, 2004). For chitosan derivatives, molecular modifications were tested for possible usage in liposomes, while the oral safety of materials needs further biological evaluation. This concerns in particular the recommended administered dosage, because the toxicity of chitosan increases with increasing charge density of the molecule (Kean & Thanou, 2010). In view of curcumin-loaded liposomes, although several studies have illustrated the feasibility and improved stability throughout chitosan coating, only low or medium molecular weight chitosan or derivatives have been so far investigated (Cuomo et al., 2018; Karewicz et al., 2013; Liu et al., 2015).

To address this issue, we undertook an evaluation study on low and high molecular weight chitosan used in the preparation of Cur-LP by the thin film hydration method. Additionally, low, medium and high concentrations of each chitosan were investigated.

125 A library of Cur-LP coated with chitosan was prepared for stability and *in vitro* release

126 performance comparisons, such as environmental stress (salt, light, and heat) and long-

127 term storage. We illustrate how molecular weight and different concentrations

128 modulate the stability and release profile of Cur-LP, with promising results for the

129 development of chitosan-coated liposomes for potential applications in healthcare

130 products and drug therapy in the future.

131

132 **2. Materials and methods**

133 *2.1 Materials and chemicals*

134 Soybean lecithin (Lecigran 1000P, powdered soybean lecithin containing a

135 mixture of phospholipids, such as phosphatidylcholine, phosphatidylethanolamine and

136 phosphatidylserine; acetone insoluble substance content > 96%) was obtained from

137 Cargill Asia Pacific Food System Co., Ltd (Beijing, China). Curcumin (> 95% purity)

138 was obtained from Hebei Food Additive Co., Ltd (Hebei, China). Cholesterol was

139 purchased from the Sinopharm Chemical Reagent Co., Ltd (Shanghai, China). Chitosan

140 with low molecular weight (MW=50-190 kDa, deacetylation degree > 75%) and high

141 molecular weight (MW=310-375 kDa, deacetylation degree > 75%), pyrene ($\geq$ 99%),

142 1,6-Diphenyl-1,3,5-hexatriene (DPH, 98%), mucin from porcine stomach (M2378),

143 pepsin from porcine gastric mucosa (P7125, enzymatic activity $\geq$ 400 units/mg protein),

144 pancreatin from porcine pancreas (P1750, 4 × USP) and bile salts were purchased from

145 Merck (Shanghai, China). Triton X-100 was purchased from Xi Long Chemical Co.,

146   Ltd (Guangzhou, China). All other reagents used were analytical grade without further

147   purification.

148   *2.2 Preparation of Cur-LP coated with chitosan*

149   Cur-LP was prepared by the thin film hydration method combined with high-

150   pressure homogenization, which reduces the vesicle size and improves the liposomal

151   homogeneity. The chloroform solvent containing soybean lecithin, cholesterol, and

152   curcumin (5:1:0.125, w/w/w) was vacuum-desiccated on a rotary evaporator to form a

153   thin lipid film over the inside surface of a round-bottom flask. This procedure lasted for

154   at least 30 min in order to remove residual chloroform. Then, the lipid film was hydrated

155   with acetate buffer (0.05M, pH 5.0) and subjected to weak sonication for eluting the

156   film easier. The obtained coarse liposome suspension was homogenized using high-

157   pressure homogenization (80 MPa, three cycles) for decreasing the vesicle sizes of Cur-

158   LPs. The fortified concentration of soybean lecithin was 10 mg/mL.

159   The prepared Cur-LP dispersion was added dropwise into LCS and HCS solution

160   (dissolved in the same acetate buffer described above) by peristaltic pump at the volume

161   ratio of 3:5 combined with magnetic stirring for 60 min. The dropping speed was 2.5

162   mL/min. Based on the pre-set gradient concentrations of each chitosan (1, 2.5 and 5

163   mg/mL, respectively), final concentrations of chitosan were diluted to 0.625, 1.563 and

164   3.125 mg/mL after mixing with Cur-LP dispersion. These three concentrations are

165   referred to as low (L), medium (M) and high (H) concentration of chitosan. Accordingly,

166   LCS-L (-M, -H) and HCS-L (-M, -H) define Cur-LP coated by low and high molecular

167 weight chitosan with low (medium, high) concentrations. Respectively. Chitosan-

168 coated Cur-LP was stored in refrigerator at 4 °C for further analysis.

2.3 The vesicle characterization of liposomes

170 The vesicle size, zeta potential, and size distribution were determined by dynamic

171 light scattering (DLS) using Malvern ZetasizerNano-ZS90 (Malvern Instruments Ltd.,

172 UK). Samples were 10-fold diluted with acetate buffer for fear of the multiple scattering

173 that influences the data accuracy. Each sample was equilibrated in the instrument for 2

174 min before test.

175 The encapsulation efficiency (EE) of curcumin in liposomes was determined by

176 absorbance using UV-1800 spectrophotometer (Shimadzu, Japan). Firstly, liposomes

177 were centrifuged ($15000 \times g$) to remove the probably absorbed or dissociated curcumin

178 on the vesicle surfaces or medium. The sedimentation was re-dispersed by buffer and

179 centrifuged again. This procedure was repeated for three times to remove the

180 unembedded curcumin as much as possible. Finally, the sedimentations were disrupted

181 by Triton X-100 and methanol, and the originally encapsulated curcumin dissolved in

182 methanol was detected by its absorbance band at 428 nm. Primary Cur-LP was treated

183 in the same way as sedimentation described above for determining the gross amount of

184 curcumin. The EE of curcumin was calculated using the following equation:

$$EE(\%) = \frac{\text{Amount of encapsulated curcumin}}{\text{Total amount of curcumin}} \times 100 \qquad (1)$$

2.4 TEM

187   The microstructures of liposomes were observed by JEM-1200EX transmission

188   electron microscope (TEM, Japanese Electronics Co., Ltd, Japan). The freshly prepared

189   liposomes, which were diluted beforehand, were transferred on a 200-mesh carbon-

190   coated copper grid. Then, samples were negatively stained by uranyl acetate solution

191   (3%) for 90 s and air-dried at room temperature. Excessive liquid could be removed

192   using filter paper if necessary. TEM images of liposomal vesicles were captured at an

193   accelerating voltage of 100 kV.

194   *2.5 Stability studies*

195   *2.5.1   Salt stability*

196   The stability of liposomes against salts stress was evaluated by incubating them in

197   NaCl solutions with different concentrations (100-1000 mM) at room temperature for

198   1 h. The relative change rate of vesicle size (ΔS) and net zeta potential (ΔP) were

199   calculated using the following equation:

200    $$\Delta S(\Delta P) = \frac{\text{Vesicle size (|zeta potential|) after incubation}}{\text{Vesicle size (|zeta potential|) in initial}} \times 100 \qquad (2)$$

201   *2.5.2   Photo stability*

202   All liposomes were transferred into transparent glass tubes and sealed by rubber

203   stoppers. The simulated solar irradiation was performed using a xenon test chamber (Q-

204   SUN, Xe-1-B, Q-Lab Corporation, Ohio, USA) for 6 h. At predetermined irradiation

205   time, an aliquot of treated sample was adequately dissolved into anhydrous methanol

206   followed by centrifugation. The supernatant was collected to determine the

207   concentration of residual curcumin in samples by absorbance. The curcumin retention

rates (%) after different periods of irradiation were calculated using the following

equation:

$$\text{Curcumin Retention (\%)} = C_t / C_0 \times 100 \tag{3}$$

Where C_0 and C_t are concentrations of curcumin in initial and in different sampling

time, respectively.

2.5.3   Thermal stability

The thermal stability of Cur-LP was evaluated at 80 °C in a water bath combining

light avoidance. Similar to the operation in photo stability evaluation, samples taken at

pre-set time intervals were also mixed with anhydrous methanol. After centrifugation,

the absorbance of collected supernatant was measured by UV-vis spectrophotometry at

428 nm. The retention rates (%) of curcumin after different periods of heat treatment

were calculated using the equation in photo stability evaluation.

2.5.4   Centrifugal stability

The centrifugal stability of liposomes was evaluated by a multi-sample analytical

centrifuge LUMiSizer® (L.U.M GmbH, Berlin, Germany), which determines the

physical stability by detecting the dynamic change of transmission intensity of

dispersions in test tubes in terms of time and position. The evolution of transmission

profile shows a continuously changing instability process during centrifugation, such

as the vesicle migration and sedimentation. In this study, all liposomes were subjected

to centrifugation at speed of 2000 rpm for 1 h. A total of 360 profiles were recorded in

intervals of 10 s. Furthermore, the instability index was recorded by the SEPView®

229   software (L.U.M, Berlin, Germany), which can intuitively compare the differences of

230   instability between samples during centrifugation.

231   *2.5.5   Storage stability*

232   All curcumin-loaded liposomes were transferred into the sealed brown glass bottles

233   and stored at 4 °C for three weeks. The vesicle sizes and residual amounts of curcumin

234   in samples were monitored at scheduled time intervals during storage, the latter was

235   calculated using the same method and equation in section 2.5.2.

236   *2.6 The determination of membrane properties*

237   *2.6.1   Micropolarity in membranes*

238   Pyrene has high sensitivity to the environmental polarity which can be used to

239   manifest the order degree of molecular arrangement in membranes. Briefly, the pyrene

240   solution (2 mM in acetone) was mixed with liposomes (10-fold diluted) at a volume

241   ratio of 1:50. The mixture was vortexed and incubated overnight at 4 °C. The

242   fluorescence emission spectra ranging from 350 to 450 nm was collected using F-7000

243   fluorescence spectrophotometer (Hitachi High-Technologies, Tokyo, Japan) at the

244   excitation wavelength of 338 nm. The fluorescence intensity ratio (I_1/I_3) of first and

245   third pyrene monomer vibronic peak was calculated. A higher ratio value means higher

246   polarity.

247   *2.6.2   Fluidity of membranes*

248   As a rod-shaped fluorescence probe, DPH inserted into liposomal membranes was

249   tightly immobilized by adjacent phospholipid molecules. Hence, the inclination degree

12

250   of DPH caused by the undulation of membranes can be used to manifest the fluidity

251   degree. This is called 'polarization (P)', which is independent of pyrene concentration.

252   The DPH solution (2 μM in dimethyl sulfoxide) and liposome (10-fold diluted) were

253   mixed at the volume ratio of 1:5. The mixture was incubated at room temperature for

254   60 min. The wavelength of excitation and emission were 360 nm and 430 nm,

255   respectively. The emission intensities were collected from directions perpendicular and

256   parallel to the exciting light. The polarization of DPH was calculated using the

257   following equations:

258          $P = (I_{0,0} - G \times I_{0,90})/(I_{0,0} - G \times I_{0,90})$ (4)

259   With $G = I_{90,0}/I_{90,90}$ (5)

260   where $I_{0,0}$, $I_{0,90}$, $I_{90,0}$, $I_{90,90}$ are fluorescence intensities of emitted light (exciting light)

261   polarized to exciting light (emitted light) in parallel (0) and vertical (90), respectively.

262   G is the grating correction coefficient. The fluorescence intensity of DPH in the

263   aqueous phase is almost non-detectable.

264   *2.7 The release assay in vitro simulated digestion*

265   *2.7.1   The protocol of in vitro simulated digestion*

266   *In vitro* simulated gastrointestinal tract (GIT) model was established to reveal the

267   effects of molecular weight and concentration of chitosan on the release characteristics

268   of curcumin in chitosan-coated liposomes. It included mouth phase (simulated saliva

269   fluid, SSF, pH=6.8), gastric phase (simulated gastric fluid, SGF, pH=1.5) and small

270   intestine phase (simulated intestinal fluid, SIF, pH=7.0) according to our previous study

271 (Tai et al., 2019). The whole simulated digestion process was carried out in a water bath

272 shaking at 37 °C. All simulated digestive juices and liposomes should be preheated at

273 37 °C before mixing together. The detailed *in vitro* simulated digestion operation as

274 follows:

275 Simulated mouth digestion was mixing liposomes with SSF (1:1, v/v) and took for

276 10 min. SSF was prepared by dissolving NaCl (1.594 g), KCl (0.202 g), and mucin (0.6

277 g) into 1 L of distilled water.

278 Simulated gastric digestion was mixing oral digestion with SGF (1:1, v/v) and took

279 for 2 h. SGF was prepared by dissolving NaCl (2 g), concentrated HCl (7 mL), and

280 pepsin (3.2 mg/mL) into 1 L of distilled water.

281 Simulated small intestine digestion was mixing stomach digestion with SIF (1:1,

282 v/v) and took for 2 h. SIF was prepared by dissolving K_2HPO_4 (6.8 g), NaCl (8.775 g),

283 bile salts (5 g), and pancreatin (3.2 mg/mL) into 1 L of distilled water. It was noteworthy

284 that the pH of stomach digestion must be adjusted to 6.8-7.0 before mixing with SIF.

285 *2.7.2   The determination of release profiles*

286 The release property of curcumin from chitosan-coated liposomes was

287 investigated by monitoring its release rate at predetermined time intervals during

288 simulated digestion. 500 µL of digestive mixture was withdrawn from each phase and

289 cooled down under an ice bath. For quantitative analysis of curcumin, the digestive

290 mixture was centrifuged at $15000 \times g$ for 30 min at 4 °C. The supernatant was collected

291 to analyse the released amount of curcumin by absorbance. Note that, the release

292   amount of curcumin should be calculated by subtracting the free curcumin in initial

293   without simulated digestion. The cumulative release rate (%) of curcumin was plotted

294   as a function of time as follows:

295    $$\text{Cumulative release(\%)} = \Sigma_0^t\left(\frac{M_t}{M_0}\right) \times 100 \qquad (6)$$

296   where M_0 and M_t are the initial amount of curcumin in liposomes without digestive

297   treatment and the cumulative amount of released curcumin for each sampling in

298   digestive medium, respectively.

299   *2.8 Statistical analysis*

300   All experiments were carried out in triplicate and data were expressed as mean ±

301   standard deviation. One-way ANOVA and Duncan's significant difference test at 5%

302   level of significance by IBM SPSS software version 25 (IBM Corp., NY) were

303   performed. Data were processed using Origin 9.0 (OriginLab Inc., Northampton, MA,

304   USA).

305

306   **3.   Results and discussion**

307   *3.1 Characteristics of chitosan-coated Cur-LP*

308   The vesicle characteristics and encapsulation efficiencies of different chitosan-

309   coated Cur-LP are summarized in Table 1, size distributions and TEM images are

310   shown in Fig. 1. Compared with uncoated Cur-LP, the chitosan coating obviously

311   increased the mean vesicle size of liposomes, but polydispersity index (PDI) result

312   displayed opposite trends. The negatively charged Cur-LP (-45 mV) was changed to be

15

313 positive, when chitosan coating was introduced. It powerfully demonstrated the

314 successful coating of chitosan onto liposomal vesicles by electrostatic interaction

315 between the positively charged amine (NH_3^+) groups of chitosan and negatively

316 charged polar head groups of phospholipids (Henriksen et al., 1994; Zhou et al., 2018).

317 Because of no significant differences of zeta potential among different chitosan-coated

318 Cur-LP, the surfaces of liposomes can be thought of as completely covered by chitosan

319 in this study. As for concentration of chitosan, the vesicle size of Cur-LP increased with

320 the increase of chitosan concentration except for LCS-H. Generally, the results suggest

321 that higher chitosan concentration induce larger self-assembled aggregates on the

322 liposomal surfaces, which in turn lead to a thicker coating layer (Park et al., 2014). This

323 trend is also seen for HCS coatings, inducing even larger molecular aggregates that

324 leads to overall larger vesicle sizes. The exceptionally smaller size of LCS-H coated

325 liposomes can be attributed to the stronger hydrophobic character of LCS at higher

326 concentration (Tan et al., 2013). In this case, high concentrations cause chitosan to self-

327 aggregate in the buffer, leading to a partial dissociation phenomenon of the chitosan

328 layer. We note, that the different molecular weight and viscous property for HCS

329 eradicates this dissociation effect at higher concentrations (Pavinatto, Caseli, &

330 Oliveira, 2010). Laye et al. have investigated the relationship between chitosan

331 (medium molecular weight) concentration and vesicle size in bare liposomes. They

332 found that the vesicle size of chitosan-coated liposomes increased gradually, when the

333 chitosan concentration was greater than 0.5 mg/mL. The vesicle size was about 1000

334   nm when the concentration was 2 mg/mL (Laye et al., 2008), which is consistent with

335   our results.

336   Although liposomes already had a satisfactory encapsulation capacity for curcumin

337   with EE reaching up to 82% in this study, which is similar with result of a previous

338   study (about 80%) (Choudhary, Shivakumar, & Ojha, 2019), the chitosan coating led

339   to a clearly increased EE ranging from 95 to 99% (Table 1). We note, that for the

340   different chitosan coatings with low and high molecular weight, no particular

341   concentration dependence was observed (2% and 3% variation in EE for low and high

342   molecular chitosan coatings, respectively; Table 1), and only slightly higher EE values

343   were determined for HCS-coated liposomes compared with LCS-coated ones. Similar

344   results were obtained in a study of resveratrol-loaded liposomes coating by chitosan

345   (Park et al., 2014). Different results were obtained by Tan showing that chitosan coating

346   slightly increased the EE of carotenoid in dependence of chitosan concentration (Tan,

347   Feng, Zhang, Xia, & Xia, 2016). Slight reduction or disparities in EE with varying

348   chitosan concentration might be attributable to liposomes coalescence during the

349   centrifugation step (Li, Paulson, & Gill, 2015).

350   As shown in Fig.1, all Cur-LP display spherical shapes and coating layers are

351   clearly observed in the formation of core-shell structures. Moreover, vesicles of all

352   chitosan-coated Cur-LP dispersed well, apart from LCS-L sample, in which some

353   bridging among vesicles appeared. Increasing chitosan concentration led to

354   monodisperse suspension at the highest chitosan concentration.

355 *3.2 The stability studies*

356 *3.2.1 Salt stability*

357   Salt is commonly used as dietary sodium supplement in food product. Thus, it is

358 essential to evaluate stability of liposomes subjected to salt solution with a gradient

359 concentrations, which is shown in Fig. 2. The relative change rate of liposomal vesicle

360 size was calculated for comparison. When NaCl concentration was below 200 mM, the

361 decreased vesicle size were observed for all liposomes. This is mainly attributed to a

362 decrease of electrostatic interaction between chitosan and liposomes caused by

363 electrostatic screening effect of NaCl, and consequently, partial dissociation of chitosan

364 from the surfaces of liposomes appeared (Liu et al., 2016). The corresponding zeta

365 potential changes are shown in Fig. S1. However, as NaCl concentration is further

366 increased, the vesicle size increases for Cur-LP, LCS-L and LCS-M. In particular, the

367 LCS-L coated vesicles increases in size more than twice compared to Cur-LP at 600-

368 1000 mM. A similar phenomenon was also obtained by the group of Cheng (Cheng et

369 al., 2017). The vesicle size of Cur-LP prepared by the same method exhibited first a

370 decrease followed by an increase in size as NaCl concentration further increased. Our

371 study further found that both LCS and HCS at high concentrations improve the salt

372 stability of Cur-LP. Note, that also the vesicle size variation as a function of salt

373 concentration decreases. Concluding, larger molecular weight and higher concentration

374 of chitosan render Cur-LP less sensitive to changes in salt concentration.

375 *3.2.2 Photo stability*

376   Due to the photosensitivity of curcumin, solar radiation is an important factor to

377   consider, especially when it comes to long-term storage and shelf-life. In our previous

378   study, the incorporation of β-sitosterol in Cur-LP improved the photo stability to some

379   extent, when compared to liposomes without sterol (Tai, et al., 2019). In this study, the

380   protective effect of chitosan on light degradation of encapsulated curcumin in

381   liposomes was evaluated in terms of molecular weight and concentration. As shown in

382   Fig. 3, the retention rate of curcumin in Cur-LP was much lower than chitosan-coated

383   ones, which demonstrates that the protection of chitosan-covered vesicles works well

384   for curcumin. We attribute the firm barrier formed by chitosan to improve the

385   encapsulation properties of liposomes, and hence, make it harder to irradiate curcumin.

386   Similarly, polyethylene glycol (PEG) coated on liposomes were also proved to

387   effectively reduce light degradation of encapsulated doxorubicin (Bandak, Ramu,

388   Barenholz, & Gabizon, 1999). Further, chitosan with different molecular weights have

389   different protective effects on photo stability of Cur-LP. HCS protected curcumin from

390   light degradation better than LCS as reflected in the higher retention rate of curcumin

391   (Fig. 3). For the significantly different curcumin retention performance between LCS

392   and HCS, we speculate that LCS does not form a uniformly-coated layer, whereas

393   protective HCS layers are expected to display a better surface coverage (Desai, Liu, &

394   Park, 2006). We note, that some aggregations were observed in TEM image for LCS-

395   L, which worsened the leakage of curcumin. In conclusion, the thicker chitosan coating

396   formed by HCS in combination with increasing concentrations reduces Cur-leakage. A

397 similar result was obtained by Li showing that HCS coatings performed better at

398 protecting curcumin in emulsion (Li, Hwang, Chen, & Park, 2016). With respect to

399 energy absorption by sunlight irradiation, also the thermal stability of chitosan-coated

400 liposomes was investigated to further verify the barrier effect of chitosan coatings.

401 *3.2.3   Thermal stability*

402   It is obvious that thermal sensitivity for curcumin and high temperature applied in

403 food products manufacturing like sterilization are irreconcilable. Therefore, an

404 enhanced thermal stability is favourable to practical curcumin products. It has been

405 proven that chitosan coating markedly protected curcumin from thermal degradation in

406 liposomes (Liu et al., 2015). Concerning our work, the thermal stability of Cur-LP

407 coated by LCS and HCS with different concentrations is shown in Fig. 4. Compared

408 with the rapid decrease of curcumin retention rate for Cur-LP, where less than 60% of

409 curcumin remained after 60 min, all chitosan-coated Cur-LP displayed better thermal

410 stability, in which curcumin retention rates were over 80% after 60 min. Moreover,

411 chitosan with higher molecular weight and concentration improved the thermal stability

412 of Cur-LP. Particularly, more than 95% of curcumin was preserved in HCS-M or HCS-

413 H coated liposomes after heat treatment. As previously reported, when liposomes go

414 through the main phase transition, the coexistence of gel and fluid-crystalline phases

415 lead to an increased membrane permeability, which induces the leaking out of curcumin

416 (Hayashi, Kono, & Takagishi, 1998). The previous thermal and irradiation stability

417 study emphasizes though that the barrier formed by chitosan coating conserves the

418 integrity of liposomal structure effectively and also maintains the stability of embedded

419 curcumin (Tan, Feng, et al., 2016). Here, the relatively strong electrostatic interaction

420 and steric hindrance effect provided by chitosan layers make major contributions to

421 stability. A similar protective effect was reported for chitosan-coated carotenoids-

422 loaded liposomes (Tan, Feng, et al., 2016). However, protection effects in this study

423 reached its saturation already at medium level concentrations, especially for HCS

424 coatings on liposomal surfaces and led no significant improvement in protection effects.

425 *3.2.4   Storage stability*

426   All prepared Cur-LP were kept in the refrigerator for monitoring the change rate of

427 vesicle size during three weeks storage, which is shown in Fig. 5. In the absence of

428 chitosan coating, vesicle size of Cur-LP increased dramatically in the first four days

429 and remained steady after that. On the contrary, LCS-L displayed a strong decrease in

430 vesicle size at the same time. Smaller vesicle size decrease were observed for LCS-M

431 and LCS-H coatings. This trend is mainly attributed to the partial dissociation of

432 chitosan from liposomal surfaces (Han, Shin, & Ha, 2012). In contrast, high

433 concentrations of chitosan suppressed this phenomenon and the smallest size variations

434 appeared in HCS-H coated liposomes. The initial increase of HCS-coated vesicle shows

435 that a firmer coating structure was formed in the beginning, even if the same size

436 decrease trend was observed afterwards. Two principle explanations can be contributed

437 to the initial size increase: one is the aggregation of small liposomal vesicles to form

438 uniform large aggregates (Li et al., 2015); another is seen in the continuous adsorption

439 of chitosan on surfaces of liposomes (Tan & Misran, 2012). Finally, the vesicle size of

440 HCS-L, HCS-M and HCS-H liposomes started to decrease on the 2nd, 7th and 14th

441 day, respectively. This further proves that chitosan with higher concentrations is

442 delaying the dissociation of coating from liposomes, which is in favour of size stability

443 of Cur-LP in storage.

444 *3.2.5   Centrifugal stability*

445   The last stability test concerned centrifugal stability of vesicles. Therefore, an

446 accelerated stability test was carried using a LUMiSizer centrifuge (Fig. 6). All

447 specimens were subjected to the same centrifugation force in the same period of time,

448 which facilitated the formation of liposomal sedimentation. As shown in Fig. 6, colours

449 of LUMiSizer transmission profiles change from red to green gradually representing

450 the dynamic changes in scanning time. The transmission rate on the top of sample cell

451 (nearby 110 nm) increased with the test time, which manifests continuous vesicle

452 migration towards the bottom of test cell. The overall increase of transmission rate

453 obtained in Cur-LP was regarded as rapid migration of vesicles to precipitation under

454 centrifugation. In contrast, clearly lower increases of transmission rate were observed

455 in chitosan-coated Cur-LP. The diverse transmission rate changes between upper and

456 lower parts of test cell, demonstrates a delay of vesicle migration. This phenomenon

457 was more significant when chitosan concentration was increased, no matter if LCS or

458 HCS. In other words, chitosan coating as well as increasing concentration effectively

459 improved physical stability of Cur-LP. Tan had also found a stability improvement of

22

460 carotenoid-loaded liposomes in the case of chitosan coating using the same detection

461 method (Tan, Feng, et al., 2016). In order to quantize the difference of stability,

462 instability index curves were determined (Fig. 6B). When a low chitosan concentration

463 was used, LCS-L vesicles were more stable than HCS-L ones. As displayed in smaller

464 curve slopes, smaller-sized vesicles move slower than bigger ones. When the chitosan

465 concentration increased to medium level, similar slope indicated almost the same

466 centrifugal stability between LCS-M and HCS-M liposomes. Above all, HCS-H

467 vesicles had the best physical stability seen in the flat transmission profile as also

468 described previously (Caddeo et al., 2013) and displayed the smallest slope in the

469 instability index curve (Fig. 6B). This results are mainly attributed to the stronger

470 repulsive hindrance between liposomal vesicles and higher viscosity caused by the high

471 molecular weight of chitosan (Dammak & Sobral, 2018). As an amphiphilic

472 polyelectrolyte, chitosan combines both electrostatic and viscosifying stabilization

473 mechanisms, which slowed down vesicles movement as encountered under

474 centrifugation (Bouyer, Mekhloufi, Rosilio, Grossiord, & Agnely, 2012). In addition,

475 the viscosity of chitosan increased with its concentration and molecular weight, leading

476 to the slowest vesicles migration to the sedimentation of HCS-H coated Cur-LP. In

477 consideration of the relatively big vesicle size for HCS-coated Cur-LP, we conclude

478 that there is a clear connection between vesicle size and physical stability in chitosan-

479 coated liposomes. Increasing molecular weight and concentration of chitosan could

480 synergistically stabilize curcumin-loaded liposomes. The centrifugal stability results

481   are in good agreement with vesicle size variation results of the storage stability analysis.

482   *3.3 Liposomal membrane properties*

483   The decoration effect of chitosan mainly focused on the enhanced stability of

484   liposomes (section 3.2) in relation to the direct interaction of the coating with liposomal

485   surface. The membranes properties within the liposomes instead have been investigated

486   by two different fluorescence probe methods (section 2.6). Resulting micropolarity and

487   fluidity value of membranes are summarized in Fig. 7. As shown in Fig. 7A, the I_1/I_3

488   values decreased as chitosan concentration increased for Cur-LP. This demonstrates

489   that polar moieties decrease gradually, when more chitosan is deposited on the vesicles,

490   which is acting as a water penetration barrier (Tan et al., 2015). Hence, the highest

491   micropolarity was obtained for Cur-LP due to the absence of a chitosan barrier. That is,

492   in this case pyrene molecules were extensively perturbed by surrounding solvent

493   molecules to form ground state complexes with polar solvents (Heldt et al., 2001). The

494   lower micropolarity of HCS-L compared with LCS-L demonstrates that HCS

495   performed better in caging efficiently vesicles than LCS in case of low chitosan

496   concentration. Further, when the concentration was increased, micropolarity of LCS-

497   coated Cur-LP significantly decreased, while it was not obvious for HCS-coated ones.

498   It is speculated that HCS with longer molecular chains failed to cover the smaller polar

499   moieties on surfaces of liposomes, even when increasing its concentration. Conversely,

500   it might be easier for LCS to shield polar domains due to the smaller molecular volume,

501   which is also reflected in the stronger LCS-concentration dependence in the

502 micropolarity. Chen found that the permeability of chitosan membranes was inversely

503 proportional to its molecular weight (Chen & Hwa, 1996), which is in line with our

504 results and the interpretation that micropolarity of coated liposomal membranes are

505 more sensitive to chitosan concentration, when LCS coating was used.

506   The fluorescence polarization of DPH is indicative for membrane fluidity caused

507 by mobility and rotation of phospholipids in liposomal bilayers. All calculated

508 polarizations of chitosan-coated Cur-LP are presented in Fig. 7B. It is observed that as

509 chitosan concentration was increased, the fluidity of liposomal membranes decreased

510 as confirmed in the increased DPH fluorescence polarization, independent of the kind

511 of chitosan used. The results are explained by the hampered lateral movement of

512 phospholipids due to the membrane-inserting hydrophobic moieties of chitosan (Tan,

513 Feng, et al., 2016; Tan et al., 2013). Besides, membrane fluidities in all HCS-coated

514 vesicles being significantly lower than that of LCS-coated ones, illustrates that the

515 longer molecular chains of HCS, the greater the immobilizing of longitudinal motion

516 of phospholipid molecules becomes. Note, that at extreme chitosan concentrations

517 (over 3.0 mg/mL), it is observed that the fluidity of liposomal membranes increased

518 again, which was explained by the onset of membrane disruption on account of the

519 penetration of excessive chitosan into membrane bilayers (Tan et al., 2013). In our

520 study, however, the highest chitosan concentration applied in LCS-H and HCS-H did

521 not exceed 3.125 mg/mL, thus not observing any membrane disturbance. Another

522 reason for the observed membrane disruption by Tan could be attributed to the different

523   coating method applied, i.e. adding chitosan solution dropwise to liposomal dispersions

524   has the drawback that it might lead to membrane imperfections due to the

525   inhomogeneous chitosan absorption inevitably (Claesson & Ninham, 1992; Henriksen

526   et al., 1994). In contrast, the method of adding liposomes into chitosan solution applied

527   in this study appeared to be more favourable to make excess of chitosan polymer

528   available instantaneously (Henriksen et al., 1994), which effectively decreased the

529   membrane perturbing effects described above.

530   Based on membranes property studies, the more rigid protective layer formed by

531   chitosan was achieved when increasing the molecular weight and concentration. Hence,

532   the sufficient electrostatic repulsion and compact core-shell structure synergistically

533   improved the stability of Cur-LP against diverse environmental stresses studied above.

534   *3.4 In vitro release study in simulated digestion*

535   Improved physicochemical stability of chitosan-coated Cur-LP obtained above is

536   the premise of sustained release in digestion. Achieving progress in slow release

537   performance for encapsulated curcumin is the final objective of this study. As shown

538   in Fig. 8, since less than 4% of curcumin was released from chitosan-coated liposomes

539   or slightly over 6% from uncoated ones, the simulated mouth phase is not the primary

540   release site for liposomes due to the short duration of this digestion step and the absence

541   of any specific enzyme activity. Most of released curcumin in this phase is attributed to

542   smaller fractions liposomes being surface adsorbed and mechanical disrupted. When

543   liposomes are subjected to gastric digestion, the highest curcumin release rate was

26

544   observed in Cur-LP. Over 10% of curcumin was released in the middle of gastric

545   digestion step (75 min). Here, LCS-coated Cur-LP released more curcumin than HCS-

546   coated ones, although the release degree was still not high. It is also well verified that

547   chitosan-coated Cur-LP transport more curcumin into the major digestive site (small

548   intestine). Similar results were obtained in previous studies (Tai et al., 2017; Tan et al.,

549   2014). As expected, the greatest Cur-release took place during the simulated small

550   intestine phase for all liposomes. Cur-LP displayed the fastest release that over 80% of

551   embedded curcumin was released after 250 min digestion. The release rates of LCS-

552   coated liposomes were still higher than HCS-coated ones. Moreover, the release rate of

553   chitosan-coated liposomes was largely dependent with chitosan concentration.

554   Chitosan at higher concentrations slowed the release of curcumin from liposomes,

555   which is consistent with results of improved liposomal stability and reduced membrane

556   fluidity. The liposomal membranes coated by a strong chitosan framework protect

557   curcumin from leakage and degradation by the complex digestive environment, such as

558   digestive movement, human body temperature and various chemicals. The result of *in*

559   *vitro* simulated digestion reveals that HCS coating with high concentration (about 3

560   mg/mL) is indeed a promising strategy for further improving the sustained release

561   properties of Cur-LP.

562

563   **4. Conclusions**

564   In this study, we provide a systematic *in vitro* stability evaluation for Cur-LP coated

565 by chitosan in terms of different molecular weights and concentrations. Apart from the

566 proved protective effect of chitosan on liposomes in previous studies, this study further

567 reveals that molecular weight and concentration of chitosan play an important role in

568 stabilizing Cur-LP. Both, LCS and HCS coating resulted in better photo and thermal

569 stability, especially for high concentration. As to the storage and centrifugal stability

570 test, increasing chitosan concentration is verified as an effective method in improving

571 stability. The membrane properties studies reveals that the liposomal membranes

572 become more rigid and compact, if molecular weight and concentration of chitosan was

573 increased. The reduced membrane fluidity effectively decreased membrane disruption

574 and leakage of curcumin from the liposomes. This is understood to be the main reason

575 for HCS-H coated liposomes to display the best sustained release property in simulated

576 digestion. The positive effect of chitosan with high molecular weight and concentration

577 on *in vitro* stability is promising for the manufacturing liposomal food with longer

578 shelf-life and strongly improves bioavailability of bioactive compounds as shown for

579 the case of curcumin.

580

(CSC) for studying in the United Kingdom.

References

Alavi, S., Haeri, A., & Dadashzadeh, S. (2017). Utilization of chitosan-caged liposomes to push the boundaries of therapeutic delivery. *Carbohydrate Polymers, 157*, 991-1012.

Alehosseini, A., Gomez-Mascaraque, L. G., Martinez-Sanz, M., & Lopez-Rubio, A. (2019). Electrospun curcumin-loaded protein nanofiber mats as active/bioactive coatings for food packaging applications. *Food Hydrocolloids, 87*, 758-771.

Anand, P., Kunnumakkara, A. B., Newman, R. A., & Aggarwal, B. B. (2007). Bioavailability of curcumin: Problems and promises. *Molecular Pharmaceutics, 4*(6), 807-818.

Bandak, S., Ramu, A., Barenholz, Y., & Gabizon, A. (1999). Reduced UV-induced degradation of doxorubicin encapsulated in polyethyleneglycol-coated liposomes. *Pharmaceutical Research, 16*(6), 841-846.

Bouyer, E., Mekhloufi, G., Rosilio, V., Grossiord, J. L., & Agnely, F. (2012). Proteins, polysaccharides, and their complexes used as stabilizers for emulsions: Alternatives to synthetic surfactants in the pharmaceutical field? *International Journal of Pharmaceutics, 436*(1-2), 359-378.

Caddeo, C., Manconi, M., Fadda, A. M., Lai, F., Lampis, S., Diez-Sales, O., & Sinico, C. (2013). Nanocarriers for antioxidant resveratrol: Formulation approach,

607   vesicle self-assembly and stability evaluation. *Colloids and Surfaces B-*

608   *Biointerfaces, 111*, 327-332.

609   Chen, R. H., & Hwa, H. D. (1996). Effect of molecular weight of chitosan with the

610   same degree of deacetylation on the thermal, mechanical, and permeability

611   properties of the prepared membrane. *Carbohydrate Polymers, 29*(4), 353-358.

612   Cheng, C., Peng, S. F., Li, Z. L., Zou, L. Q., Liu, W., & Liu, C. M. (2017). Improved

613   bioavailability of curcumin in liposomes prepared using a pH-driven, organic

614   solvent-free, easily scalable process. *Rsc Advances, 7*(42), 25978-25986.

615   Choudhary, V., Shivakumar, H., & Ojha, H. (2019). Curcumin-loaded liposomes for

616   wound healing: Preparation, optimization, in-vivo skin permeation and

617   bioevaluation. *Journal of Drug Delivery Science and Technology, 49*, 683-691.

618   Claesson, P. M., & Ninham, B. W. (1992). Ph-Dependent Interactions between

619   Adsorbed Chitosan Layers. *Langmuir, 8*(5), 1406-1412.

620   Cuomo, F., Cofelice, M., Venditti, F., Ceglie, A., Miguel, M., Lindman, B., & Lopez,

621   F. (2018). In-vitro digestion of curcumin loaded chitosan-coated liposomes.

622   *Colloids and Surfaces B-Biointerfaces, 168*, 29-34.

623   Dammak, I., & Sobral, P. J. A. (2018). Formulation optimization of lecithin-enhanced

624   pickering emulsions stabilized by chitosan nanoparticles for hesperidin

625   encapsulation. *Journal of Food Engineering, 229*, 2-11.

626   Desai, K. G., Liu, C., & Park, H. J. (2006). Characteristics of vitamin C encapsulated

627   tripolyphosphate-chitosan microspheres as affected by chitosan molecular

weight. *Journal of Microencapsulation, 23*(1), 79-90.

Filipovic-Grcic, J., Skalko-Basnet, N., & Jalsenjak, I. (2001). Mucoadhesive chitosan-coated liposomes: characteristics and stability. *Journal of Microencapsulation, 18*(1), 3-12.

Gradauer, K., Barthelmes, J., Vonach, C., Almer, G., Mangge, H., Teubl, B., Roblegg, E., Dunnhaupt, S., Frohlich, E., Bernkop-Schnurch, A., & Prassl, R. (2013). Liposomes coated with thiolated chitosan enhance oral peptide delivery to rats. *Journal of Controlled Release, 172*(3), 872-878.

Grit, M., & Crommelin, D. J. (1993). Chemical stability of liposomes: implications for their physical stability. *Chemistry and physics of lipids, 64*(1-3), 3-18.

Han, H. K., Shin, H. J., & Ha, D. H. (2012). Improved oral bioavailability of alendronate via the mucoadhesive liposomal delivery system. *European Journal of Pharmaceutical Sciences, 46*(5), 500-507.

Hao, J. P., Guo, B., Yu, S. X., Zhang, W. T., Zhang, D. H., Wang, J. L., & Wang, Y. R. (2017). Encapsulation of the flavonoid quercetin with chitosan-coated nano-liposomes. *Lwt-Food Science and Technology, 85*, 37-44.

Hayashi, H., Kono, K., & Takagishi, T. (1998). Temperature-dependent associating property of liposomes modified with a thermosensitive polymer. *Bioconjugate Chemistry, 9*(3), 382-389.

He, H. S., Lu, Y., Qi, J. P., Zhu, Q. G., Chen, Z. J., & Wu, W. (2019). Adapting liposomes for oral drug delivery. *Acta Pharmaceutica Sinica B, 9*(1), 36-48.

649 Heldt, N., Gauger, M., Zhao, J., Slack, G., Pietryka, J., & Li, Y. (2001).

650   Characterization of a polymer-stabilized liposome system. *Reactive &*

651   *Functional Polymers, 48*(1-3), 181-191.

652 Henriksen, I., Smistad, G., & Karlsen, J. (1994). Interactions between Liposomes and

653   Chitosan. *International Journal of Pharmaceutics, 101*(3), 227-236.

654 Henriksen, I., Vagen, S. R., Sande, S. A., Smistad, G., & Karlsen, J. (1997). Interactions

655   between liposomes and chitosan .2. Effect of selected parameters on

656   aggregation and leakage. *International Journal of Pharmaceutics, 146*(2), 193-

657   203.

658 Jeon, S., Yoo, C. Y., & Park, S. N. (2015). Improved stability and skin permeability of

659   sodium hyaluronate-chitosan multilayered liposomes by Layer-by-Layer

660   electrostatic deposition for quercetin delivery. *Colloids and Surfaces B-*

661   *Biointerfaces, 129*, 7-14.

662 Karewicz, A., Bielska, D., Loboda, A., Gzyl-Malcher, B., Bednar, J., Jozkowicz, A.,

663   Dulak, J., & Nowakowska, M. (2013). Curcumin-containing liposomes

664   stabilized by thin layers of chitosan derivatives. *Colloids and Surfaces B-*

665   *Biointerfaces, 109*, 307-316.

666 Kean, T., & Thanou, M. (2010). Biodegradation, biodistribution and toxicity of

667   chitosan. *Advanced Drug Delivery Reviews, 62*(1), 3-11.

668 Laye, C., McClements, D. J., & Weiss, J. (2008). Formation of biopolymer-coated

669   liposomes by electrostatic deposition of chitosan. *Journal of Food Science,*

670   *73*(5), N7-N15.

671 Li, J., Hwang, I. C., Chen, X., & Park, H. J. (2016). Effects of chitosan coating on

672   curcumin loaded nano-emulsion: Study on stability and in vitro digestibility.

673   *Food Hydrocolloids, 60*, 138-147.

674 Li, M. Y., Du, C. Y., Guo, N., Teng, Y. O., Meng, X., Sun, H., Li, S. S., Yu, P., &

675   Galons, H. (2019). Composition design and medical application of liposomes.

676   *European Journal of Medicinal Chemistry, 164*, 640-653.

677 Li, R. W., Deng, L., Cai, Z. W., Zhang, S. Y., Wang, K., Li, L. H., Ding, S., & Zhou,

678   C. R. (2017). Liposomes coated with thiolated chitosan as drug carriers of

679   curcumin. *Materials Science & Engineering C-Materials for Biological*

680   *Applications, 80*, 156-164.

681 Li, Z. Y., Paulson, A. T., & Gill, T. A. (2015). Encapsulation of bioactive salmon

682   protein hydrolysates with chitosan-coated liposomes. *Journal of Functional*

683   *Foods, 19*, 733-743.

684 Liu, W. D., Zhai, Y. J., Heng, X. Y., Che, F. Y., Chen, W. J., Sun, D. Z., & Zhai, G. X.

685   (2016). Oral bioavailability of curcumin: problems and advancements. *Journal*

686   *of Drug Targeting, 24*(8), 694-702.

687 Liu, W. L., Liu, W., Ye, A. Q., Peng, S. F., Wei, F. Q., Liu, C. M., & Han, J. Z. (2016).

688   Environmental stress stability of microencapsules based on liposomes decorated

689   with chitosan and sodium alginate. *Food Chemistry, 196*, 396-404.

690 Liu, Y. J., Liu, D. D., Zhu, L., Gan, Q., & Le, X. Y. (2015). Temperature-dependent

691   structure stability and in vitro release of chitosan-coated curcumin liposome.

692   *Food Research International, 74*, 97-105.

693   Ma, P. H., Zeng, Q. H., Tai, K. D., He, X. Y., Yao, Y. Y., Hong, X. F., & Yuan, F.

694   (2017). Preparation of curcumin-loaded emulsion using high pressure

695   homogenization: Impact of oil phase and concentration on physicochemical

696   stability. *Lwt-Food Science and Technology, 84*, 34-46.

697   Maiti, K., Mukherjee, K., Gantait, A., Saha, B. P., & Mukherjee, P. K. (2007).

698   Curcumin-phospholipid complex: Preparation, therapeutic evaluation and

699   pharmacokinetic study in rats. *International Journal of Pharmaceutics, 330*(1-

700   2), 155-163.

701   Mujtaba, M., Morsi, R. E., Kerch, G., Elsabee, M. Z., Kaya, M., Labidi, J., & Khawar,

702   K. M. (2019). Current advancements in chitosan-based film production for food

703   technology; A review. *International Journal of Biological Macromolecules,*

704   *121*, 889-904.

705   Nelson, K. M., Dahlin, J. L., Bisson, J., Graham, J., Pauli, G. F., & Walters, M. A.

706   (2017). The Essential Medicinal Chemistry of Curcumin. *Journal of Medicinal*

707   *Chemistry, 60*(5), 1620-1637.

708   Park, S. N., Jo, N. R., & Jeon, S. H. (2014). Chitosan-coated liposomes for enhanced

709   skin permeation of resveratrol. *Journal of Industrial and Engineering Chemistry,*

710   *20*(4), 1481-1485.

711   Pavinatto, F. J., Caseli, L., & Oliveira, O. N. (2010). Chitosan in Nanostructured Thin

712 Films. *Biomacromolecules, 11*(8), 1897-1908.

713 Pu, C. F., Tang, W. T., Li, X. D., Li, M., & Sun, Q. J. (2019). Stability enhancement

714   efficiency of surface decoration on curcumin-loaded liposomes: Comparison of

715   guar gum and its cationic counterpart. *Food Hydrocolloids, 87*, 29-37.

716 Shin, G. H., Chung, S. K., Kim, J. T., Joung, H. J., & Park, H. J. (2013). Preparation of

717   Chitosan-Coated Nanoliposomes for Improving the Mucoadhesive Property of

718   Curcumin Using the Ethanol Injection Method. *Journal of Agricultural and*

719   *Food Chemistry, 61*(46), 11119-11126.

720 Tai, K., Rappolt, M., He, X., Wei, Y., Zhu, S., Zhang, J., Mao, L., Gao, Y., & Yuan, F.

721   (2019). Effect of β-sitosterol on the curcumin-loaded liposomes: Vesicle

722   characteristics, physicochemical stability, in vitro release and bioavailability.

723   *Food Chemistry, 293*, 92-102.

724 Tai, K. D., He, X. Y., Yuan, X. D., Meng, K., Gao, Y. X., & Yuan, F. (2017). A

725   comparison of physicochemical and functional properties of icaritin-loaded

726   liposomes based on different surfactants. *Colloids and Surfaces a-*

727   *Physicochemical and Engineering Aspects, 518*, 218-231.

728 Tan, C., Feng, B., Zhang, X. M., Xia, W. S., & Xia, S. Q. (2016). Biopolymer-coated

729   liposomes by electrostatic adsorption of chitosan (chitosomes) as novel delivery

730   systems for carotenoids. *Food Hydrocolloids, 52*, 774-784.

731 Tan, C., Xie, J. H., Zhang, X. M., Cai, J. B., & Xia, S. Q. (2016). Polysaccharide-based

732   nanoparticles by chitosan and gum arabic polyelectrolyte complexation as

733   carriers for curcumin. *Food Hydrocolloids, 57*, 236-245.

734   Tan, C., Xue, J., Eric, K., Feng, B., Zhang, X. M., & Xia, S. Q. (2013). Dual Effects of

735   Chitosan Decoration on the Liposomal Membrane Physicochemical Properties

736   As Affected by Chitosan Concentration and Molecular Conformation. *Journal*

737   *of Agricultural and Food Chemistry, 61*(28), 6901-6910.

738   Tan, C., Zhang, Y. T., Abbas, S., Feng, B., Zhang, X. M., & Xia, S. Q. (2014).

739   Modulation of the carotenoid bioaccessibility through liposomal encapsulation.

740   *Colloids and Surfaces B-Biointerfaces, 123*, 692-700.

741   Tan, C., Zhang, Y. T., Abbas, S., Feng, B., Zhang, X. M., Xia, S. Q., & Chang, D. W.

742   (2015). Insights into chitosan multiple functional properties: the role of chitosan

743   conformation in the behavior of liposomal membrane. *Food & Function, 6*(12),

744   3702-3711.

745   Tan, H. W., & Misran, M. (2012). Characterization of fatty acid liposome coated with

746   low-molecular-weight chitosan. *Journal of Liposome Research, 22*(4), 329-335.

747   Tian, M. P., Song, R. X., Wang, T., Sun, M. J., Liu, Y., & Chen, X. G. (2018). Inducing

748   sustained release and improving oral bioavailability of curcumin via chitosan

749   derivatives-coated liposomes. *International Journal of Biological*

750   *Macromolecules, 120*, 702-710.

751   Wang, X. Y., & Gao, Y. (2018). Effects of length and unsaturation of the alkyl chain

752   on the hydrophobic binding of curcumin with Tween micelles. *Food Chemistry,*

753   *246*, 242-248.

754   Wu, Z. H., Ping, Q. N., Wei, Y., & Lai, J. M. (2004). Hypoglycemic efficacy of

755   chitosan-coated insulin liposomes after oral administration in mice. *Acta*

756   *Pharmacologica Sinica, 25*(7), 966-972.

757   Zheng, B. J., Zhang, Z. P., Chen, F., Luo, X., & McClements, D. J. (2017). Impact of

758   delivery system type on curcumin stability: Comparison of curcumin

759   degradation in aqueous solutions, emulsions, and hydrogel beads. *Food*

760   *Hydrocolloids, 71*, 187-197.

761   Zhou, F., Xu, T., Zhao, Y. J., Song, H. X., Zhang, L. Q., Wu, X. D., & Lu, B. Y. (2018).

762   Chitosan-coated liposomes as delivery systems for improving the stability and

763   oral bioavailability of acteoside. *Food Hydrocolloids, 83*, 17-24.

764

Figure captions & Figures

Fig. 1. Vesicle size distribution of Cur-LP with and without chitosan coating. LCS and HCS represent low and high molecular weight chitosan, respectively; L, M and H represent low, medium and high concentrations of chitosan, respectively. The insert in each size distribution diagram shows the corresponding TEM image of the liposomal dispersion.

Fig. 2. Stability of Cur-LP and different chitosan-decorated Cur-LP in NaCl solution. The relative change rate of vesicle size (%) versus salt concentrations (mM) is presented.

Fig. 3. The photo stability of Cur-LP with and without chitosan coating under UV light irradiance of 0.35 W/m² for 6 h.

Fig. 4. The thermal stability of Cur-LP and chitosan-decorated ones in an 80 °C water bath for a period of one hour (10-60 min).

Fig. 5. The relative change rates of vesicle sizes for Cur-LP with and without chitosan coating during storage at 4 °C for three weeks.

Fig. 6. Transmission profiles (A1-A7) and instability index curves (B) of Cur-LP with and without chitosan coating retrieved from LUMisizer measurements at 25 °C. The profiles were recorded every 10 s for 1 h. The abscissa and ordinate in panel A1-A7 represent the test tube position and percentage of light transmission, respectively.

Fig. 7. Membrane characteristics of Cur-LP with and without chitosan coating were investigated by pyrene (A) and DPH (B) at 25 °C, respectively. Each data was expressed as the mean value ± standard deviation (n = 3).

Fig. 8. The kinetic release of curcumin from different formulations during simulated *in vitro* digestion at 37 °C. Values are presented as mean ± standard deviation (n = 3).
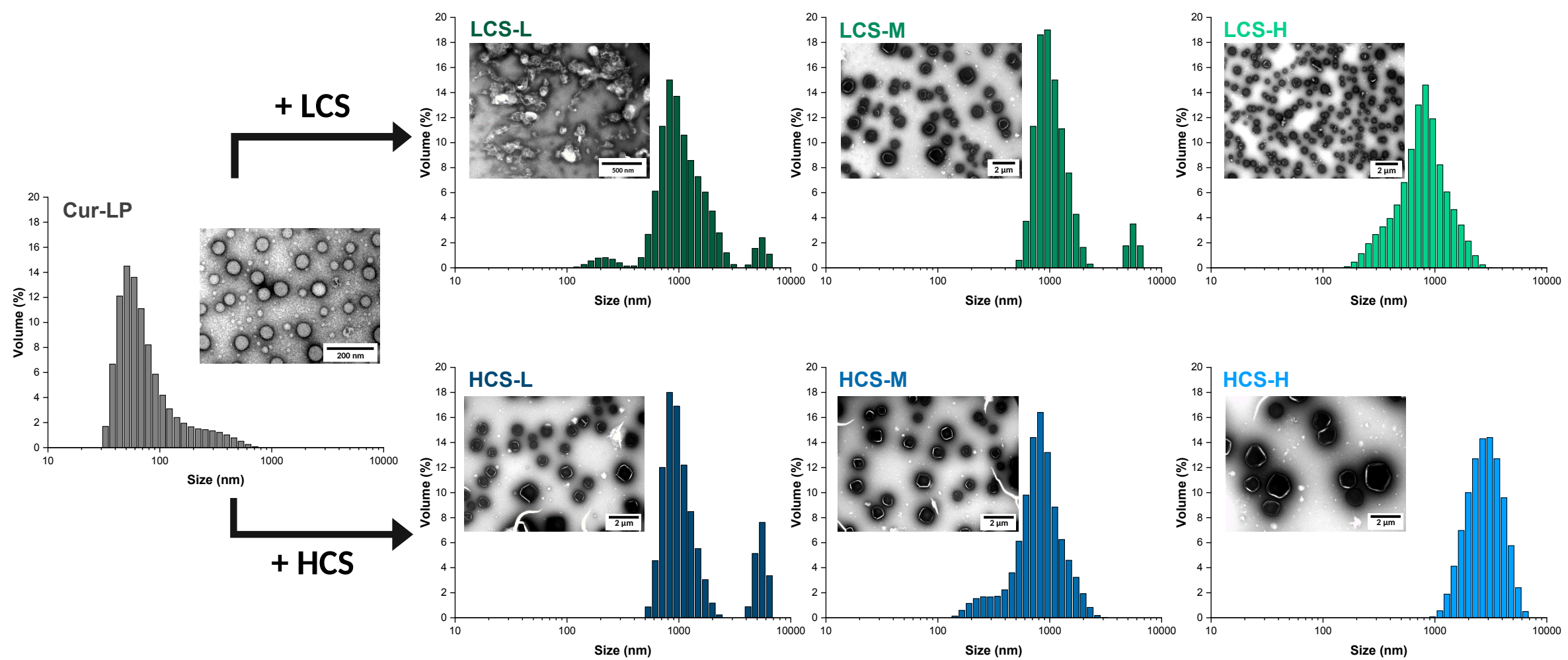
Fig. 1
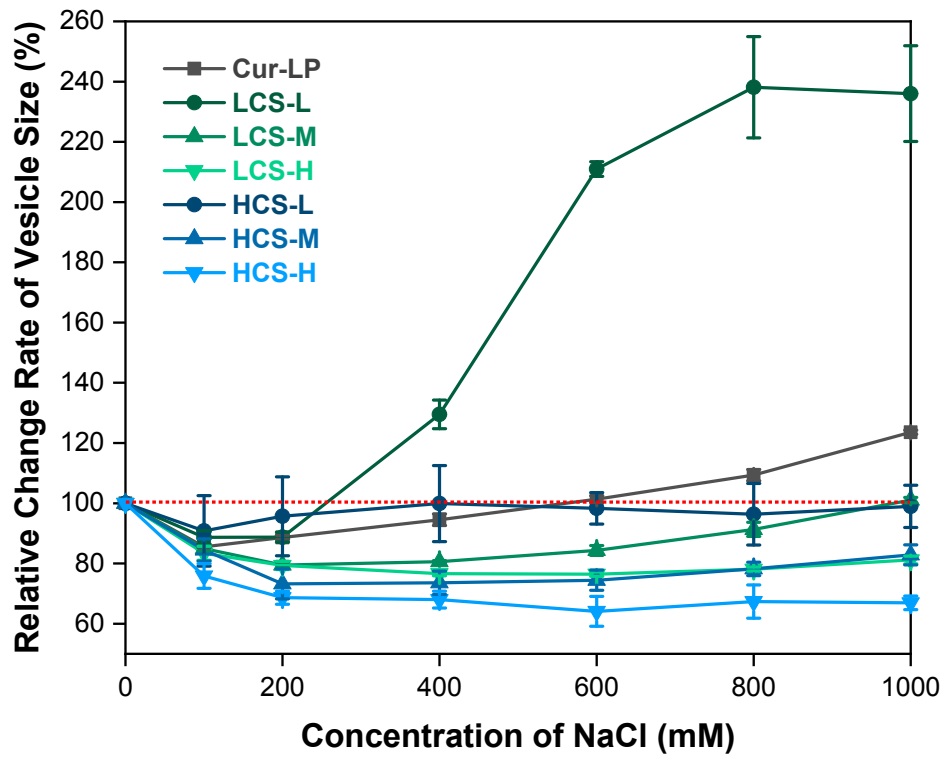
Fig. 2
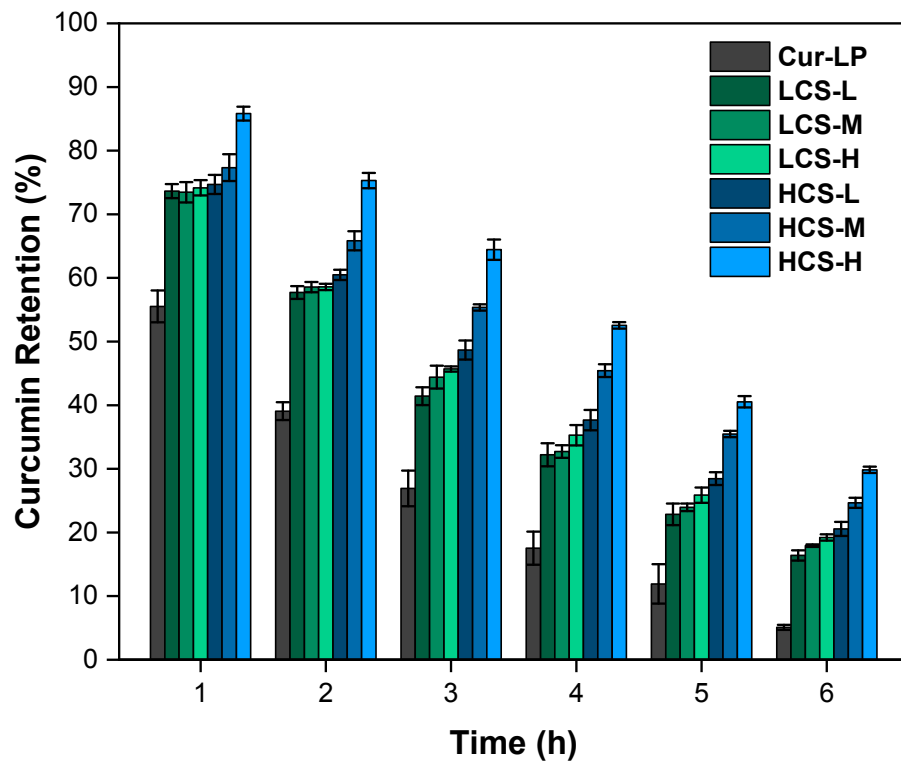
Fig. 3
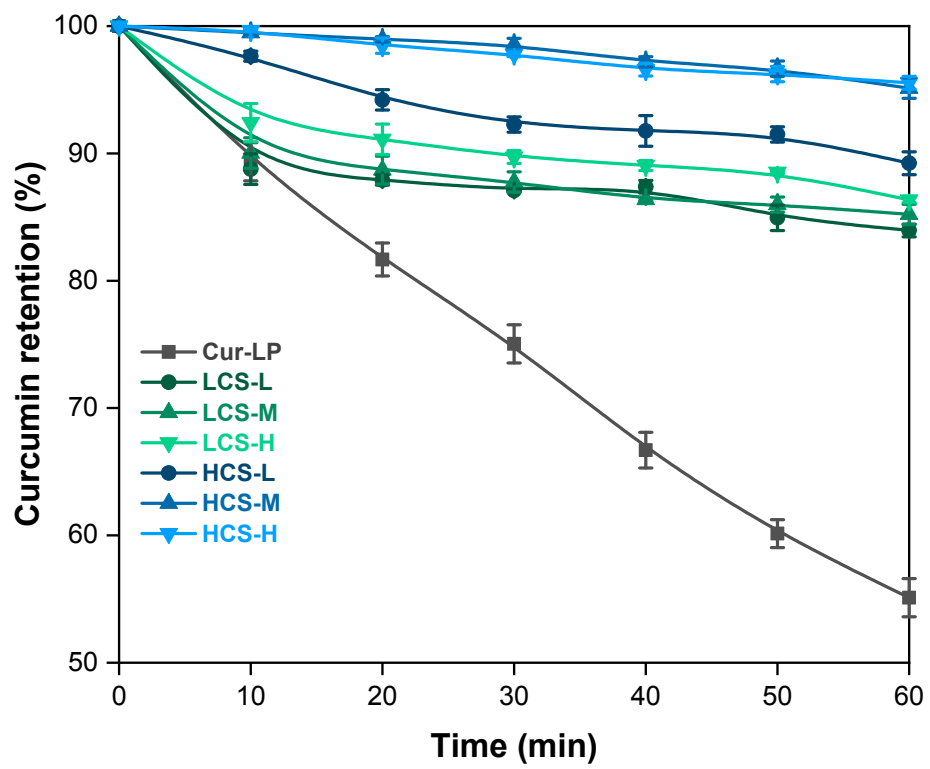
Fig. 4
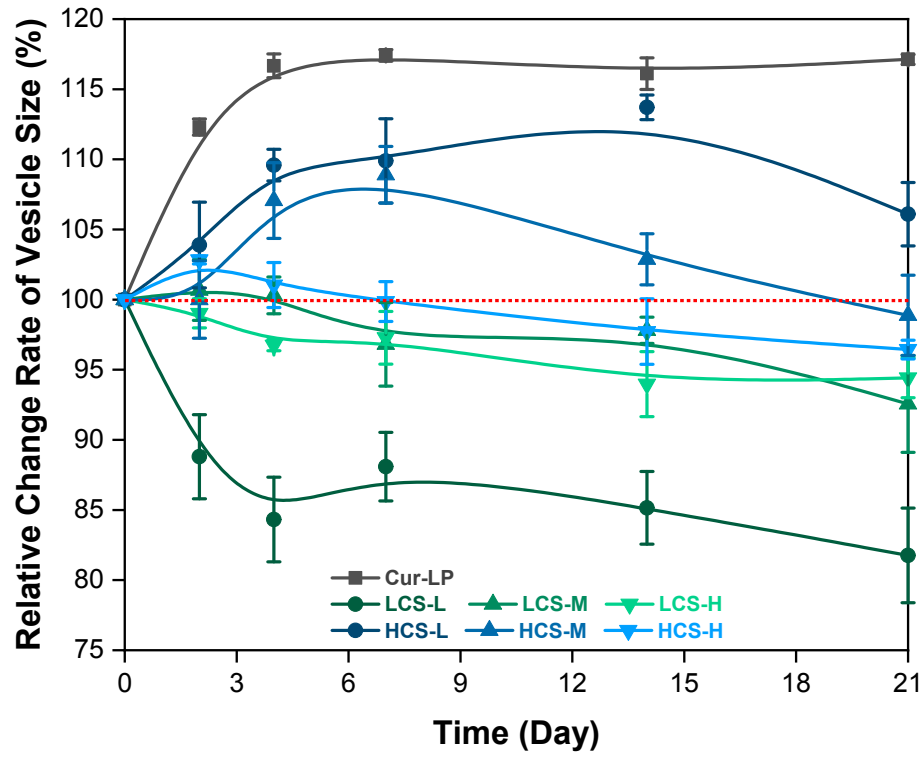
Fig. 5
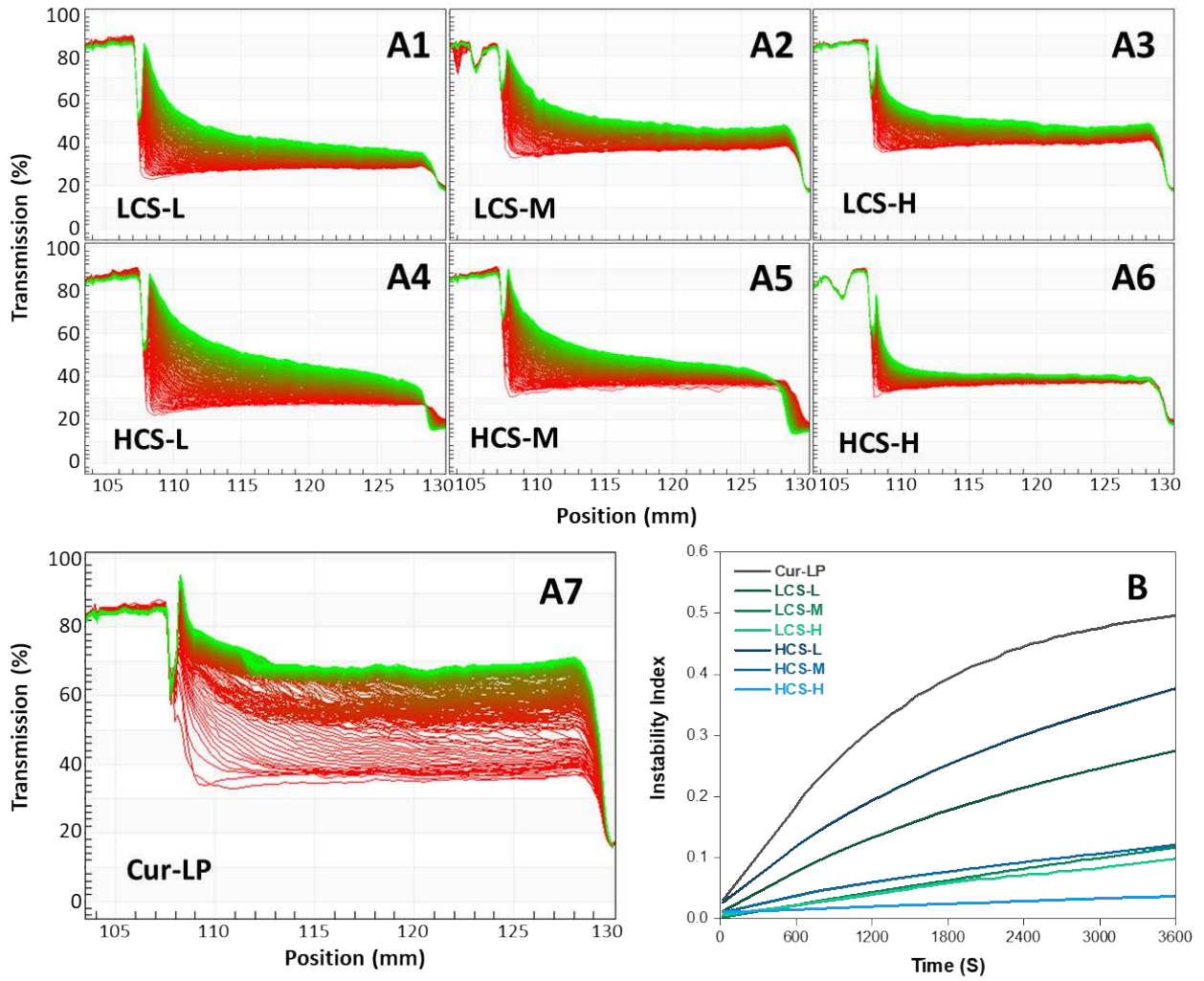
Fig. 6
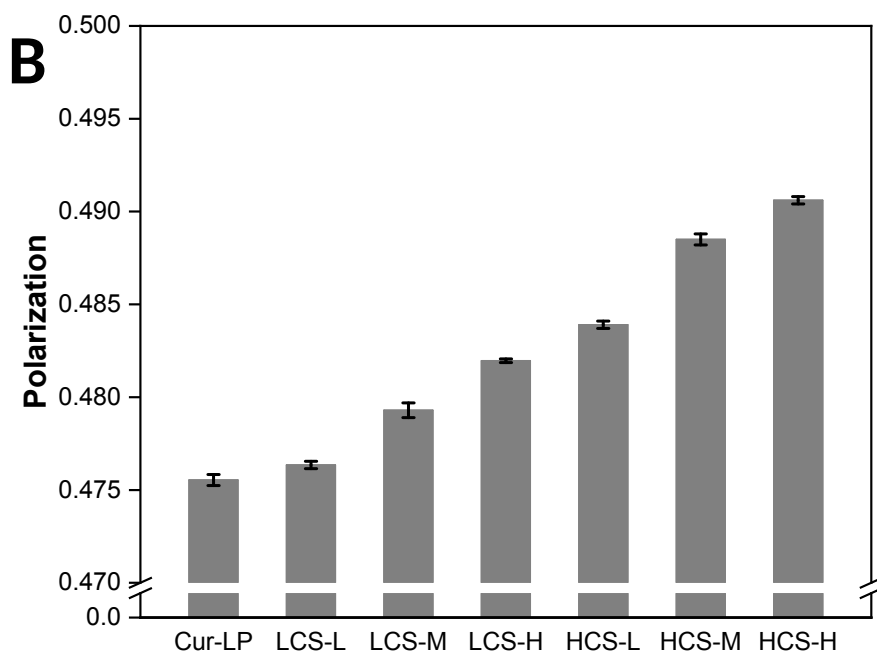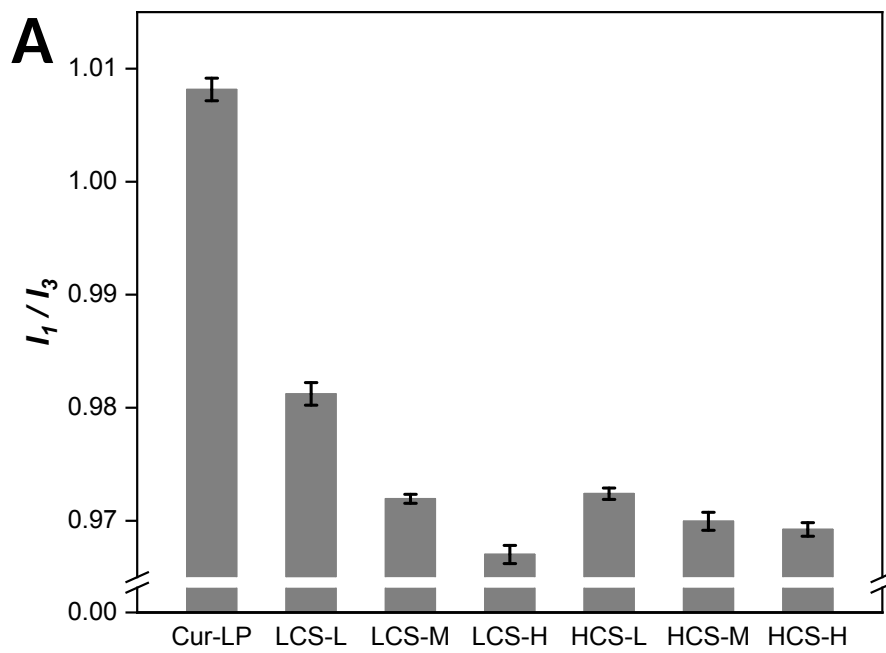
Fig. 7
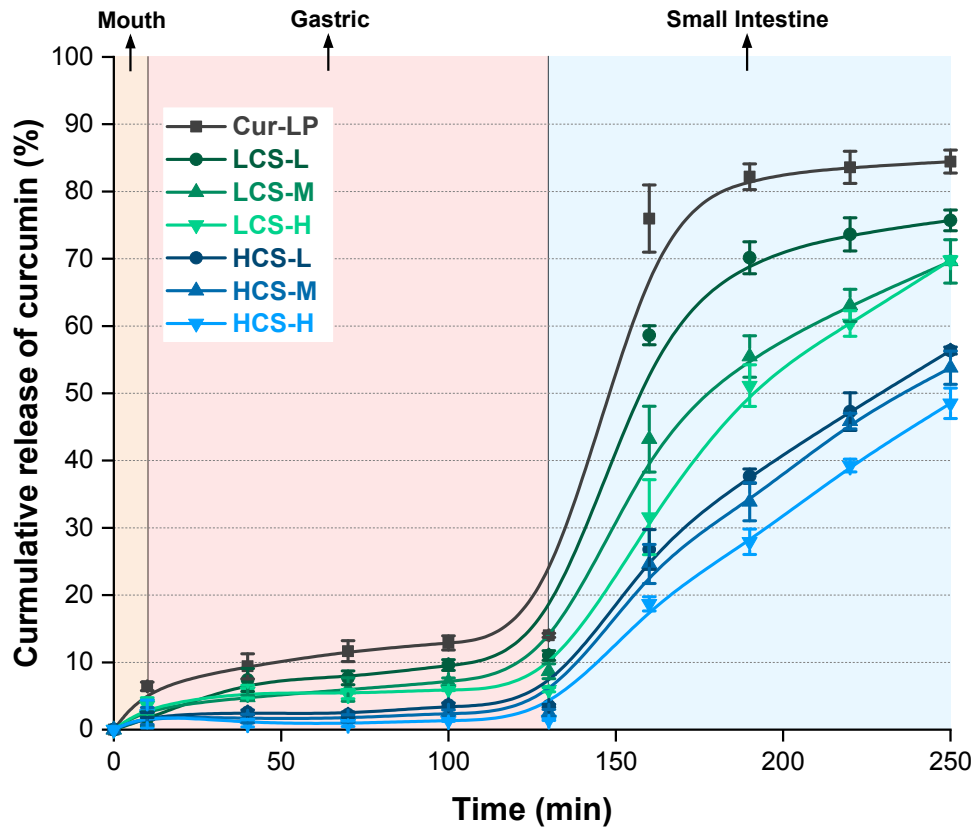
Fig. 8

TABLE CAPTIONS

Table 1. Size, polydispersity index (PDI), zeta potential and encapsulation efficiency (EE) of curcumin in different formulations.

Liposomes formulations	Vesicle size (nm)	PDI	Zeta potential (mV)	EE (%)
Cur-LP	190 ± 4	0.53 ± 0.01	-45 ± 3	82.41 ± 0.25
LCS-L	1028 ± 30	0.33 ± 0.03	36 ± 2	95.93 ± 0.61
LCS-M	1280 ± 20	0.33 ± 0.01	37 ± 2	96.66 ± 0.70
LCS-H	718 ± 7	0.33 ± 0.03	36 ± 3	94.81 ± 0.30
HCS-L	1324 ± 50	0.35 ± 0.10	36 ± 2	99.19 ± 0.26
HCS-M	1557 ± 40	0.33 ± 0.08	36 ± 2	97.55 ± 0.76
HCS-H	1729 ± 50	0.39 ± 0.11	40 ± 3	95.52 ± 0.66

Conflict of interest

Authors declare that this study does not have any conflict of interest.

Supplementary Data

The stabilization and release performances of curcumin-loaded liposomes coated by high and low molecular weight chitosan

Kedong Tai [a], Michael Rappolt [b], Like Mao [a], Yanxiang Gao [a], Xin Li [c], Fang Yuan [a,] *

[a] Beijing Advanced Innovation Center for Food Nutrition and Human Health, Beijing Laboratory for Food Quality and Safety, Beijing Key Laboratory of Functional Food from Plant Resources, College of Food Science & Nutritional Engineering, China Agricultural University, Beijing 100083, P.R. China

[b] School of Food Science and Nutrition, University of Leeds, Leeds LS2 9JT, U.K.

[c] School of Food Science, Jiangnan University, Wuxi, Jiangsu, 214122, P.R. China

* Corresponding author (Fang Yuan).

Tel: +86-10-62737034

Address: Box 112, No.17 Qinghua East Road, Haidian District, Beijing 100083, China

E-mail: yuanfang0220@cau.edu.cn

Figure S1. Stability of Cur-LP without and with different chitosan coatings in NaCl solution. The relative change rate of net potential (%) versus salt concentration (mM) is presented. Cur-LP: curcumin-loaded liposomes, LCS and HCS: low and high molecular weight chitosan, L, M and H: low, medium and high concentration of chitosan in final samples.
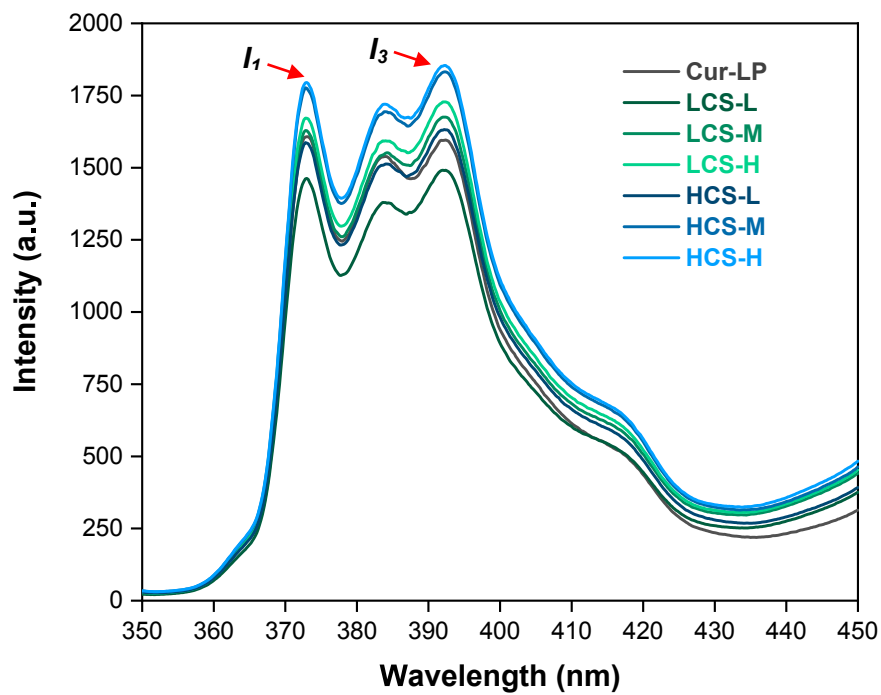
Figure S2. The fluorescence spectra of pyrene in liposomal membranes without and with different chitosan coatings. I_1 and I_3 represent the fluorescence intensity of the first and third peak in the spectra, respectively.